Reorientation Maneuver for Spinning Spacecraft

Christopher D. Rahn*
University of California, Berkeley, Berkeley, California 94720
and
Peter M. Barba†
Ford Aerospace Corporation, Palo Alto, California 94303

A spacecraft spinning about its minor axis in the presence of energy dissipation is directionally unstable. Eventually, the spacecraft will reorient to a major axis spin. After the maneuver, the major axis spin rate can be either positive or negative. Correspondingly, the orientation of the spacecraft relative to the inertially fixed angular momentum vector is unpredictable. This paper demonstrates that the maneuver, when augmented with two thruster firings based on gyro measurements, provides a desired final orientation.

Introduction

A SINGLE-body spacecraft spinning about its minor axis in the presence of energy dissipation is directionally unstable.[1] The spacecraft can be stabilized by active control, by the jet damping of a rocket motor,[2] or by dampers on a controlled, despun platform,[3] but removing these stabilizing mechanisms causes the spacecraft to reorient and rotate about its major axis due to the energy lost in fuel slosh and vibration. This passive reorientation maneuver is called spin transition.

Spacecraft may rotate about their minor axis for several reasons. First, launch vehicle fairing constraints often require that the long and narrow axis of the spacecraft be aligned with the longitudinal axis of the launch vehicle. Typically, the launch vehicle spins longitudinally prior to separation, resulting in a minor axis spin for the spacecraft after separation. Second, when a solid rocket motor raises the orbit, the rocket motor and spacecraft combination spins about its minor axis to increase stability during the firing. When the firing is completed, the combination undergoes spin transition unless active control is used.

The spin transition maneuver is subject, however, to a limitation. The orientation of the spacecraft relative to the inertially fixed angular momentum vector at the end of the maneuver cannot be determined a priori. The spacecraft can end up with either a positive or a negative major axis spin. Physically, this corresponds to two final attitudes that are 180 deg apart. Many spacecraft have sensitive onboard instruments, which must be shielded from the sun, or directional communication equipment, which must point toward the Earth. In these cases, it is desirable to ensure a final spin polarity.

There are techniques of optimally reorienting spacecraft using thrusters[4] and of acquiring attitude using momentum wheels.[5,6] In terms of fuel usage, the passive spin transition maneuver is optimal, and momentum wheels, with their attendant complexity, are not required. To make the maneuver truly useful, however, the final spin polarity must be controlled, requiring some fuel expenditure.

This paper presents a control system that guarantees a final orientation after spin transition. The control system uses gyros that determine when to fire thrusters, providing the desired orientation.

Presented as Paper AAS 89-392 at the AAS/AIAA Astrodynamics Specialist Conference, Stowe, VT, Aug. 7-10, 1989; received Sept. 18, 1989; revision received Aug. 24, 1990; accepted for publication Sept. 10, 1990.

*Graduate Student.

†Principal Engineer. Member AIAA.

Dynamics

Two models of the spacecraft dynamics are used. The analysis model consists of a rigid body with an energy sink. For simulation purposes, the spacecraft is modeled as a rigid body with a spherical, dissipative fuel slug. The rigid body has three rates ω_1, ω_2, and ω_3 about the major, intermediate, and minor body axes, respectively. The fuel is modeled as a spherical slug of inertia J, which is surrounded by a viscous layer. Designating the relative rates between the spacecraft body and the fuel slug as σ_1, σ_2, and σ_3, the equations of motion are written as

$$(I_1 - J)\dot{\omega}_1 = (I_2 - I_3)\omega_2\omega_3 + \Delta\sigma_1 + T_1 \tag{1a}$$

$$(I_2 - J)\dot{\omega}_2 = (I_3 - I_1)\omega_1\omega_3 + \Delta\sigma_2 + T_2 \tag{1b}$$

$$(I_3 - J)\dot{\omega}_3 = (I_1 - I_2)\omega_1\omega_2 + \Delta\sigma_3 + T_3 \tag{1c}$$

$$\dot{\sigma}_1 = -\dot{\omega}_1 - \Delta\sigma_1/J - \omega_2\sigma_3 + \omega_3\sigma_2 \tag{1d}$$

$$\dot{\sigma}_2 = -\dot{\omega}_2 - \Delta\sigma_2/J - \omega_3\sigma_1 + \omega_1\sigma_3 \tag{1e}$$

$$\dot{\sigma}_3 = -\dot{\omega}_3 - \Delta\sigma_3/J - \omega_1\sigma_2 + \omega_2\sigma_1 \tag{1f}$$

where Δ is the viscous damping coefficient of the slug; I_1, I_2, and I_3 are principal moments of inertia of the spacecraft

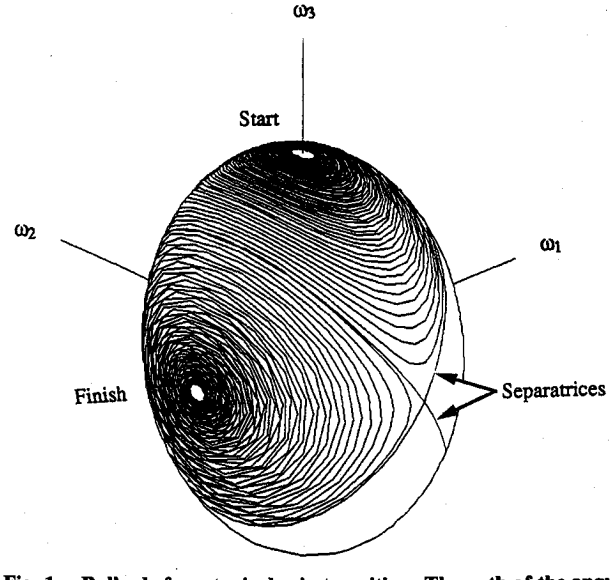

Fig. 1 Polhode for a typical spin transition. The path of the angular velocity vector in body axis coordinates starts with a positive minor axis spin and finishes with a negative major axis spin.

Table 1 Simulation parameters and initial conditions

I_1	2000 kg m^2
I_2	1500 kg m^2
I_3	1000 kg m^2
J	18 kg m^2
Δ	30 Nms
Initial major axis rate	0.1224 rad/s
Initial intermediate axis rate	0.0 rad/s
Initial minor axis rate	2.99 rad/s

including the slug; and T_1, T_2, and T_3 are torques about the principal axes. Barba et al.[7] discuss the selection of the fuel slug parameters J and Δ. The total body momentum h_v and energy T_v are expressed as

$$h_v^2 = (I_1\omega_1 + J\sigma_1)^2 + (I_2\omega_2 + J\sigma_2)^2 + (I_3\omega_3 + J\sigma_3)^2 \quad (2)$$

$$2T_v = (I_1 - J)\omega_1^2 + (I_2 - J)\omega_2^2 + (I_3 - J)\omega_3^2 + J[(\omega_1 + \sigma_1)^2 + (\omega_2 + \sigma_2)^2 + (\omega_3 + \sigma_3)^2] \quad (3)$$

The analysis model angular momentum h and rotational energy T of the rigid body can be expressed as

$$h^2 = I_1^2\omega_1^2 + I_2^2\omega_2^2 + I_3^2\omega_3^2 \quad (4)$$

$$2T = I_1\omega_1^2 + I_2\omega_2^2 + I_3\omega_3^2 \quad (5)$$

where the angular momentum and energy of the fuel slug have been neglected.

The path that the angular velocity vector traces in body axes coordinates is determined by the intersection of the momentum ellipsoid [Eq. (4)] and the energy ellipsoid [Eq. (5)] and is called the polhode. If there is no energy dissipation onboard the spacecraft, h and T are constant and the polhode is a closed path corresponding to nutational motion of the spacecraft.

If there is energy dissipation, T decreases and the energy ellipsoid shrinks with time. This leads to an open polhode path that spirals outward from the minor axis, and captures on the major axis, as shown in Fig. 1. Figure 1 is obtained by simulating Eqs. (1) with the initial conditions and parameters shown in Table 1. The viscous fuel slug provides the energy dissipation. The point at which the polhode switches from rotating about the minor axis to rotating about the major axis corresponds to crossing the separatrix.

The exact point at which the polhode crosses the separatrix is dependent on the initial conditions and the energy dissipation characteristics of the spacecraft. Small changes in either of these parameters can change the side on which the polhode crosses the separatrix, changing the final spin polarity. There is a 50% chance of capturing on either side, and it is impossible to predict.

Figure 2 demonstrates the sensitivity of the final spin polarity to initial conditions. The horizontal axis is the initial major axis spin rate and the vertical axis is the initial intermediate axis spin rate. The initial minor axis spin rate is calculated to give a constant 3000-Nms angular momentum. The figure represents a 101 × 101 grid of simulations over a typical range of rates with the X corresponding to a positive final spin. The simulation in Fig. 1 is marked with a •. A small change in the initial conditions can lead to a change in the final spin polarity.

Final Spin Polarity Control

The desired final spin polarity is guaranteed with the following control logic. Initially, the spacecraft spins about its minor axis with some small amount of nutation. The spacecraft begins to transit to flat spin, and when the polhode crosses the separatrix, the spin direction is determined. If the spin direction is correct, no action is taken. If the spin direction is incorrect, a thruster fires to force the polhode to cross the separatrix. Then, a short time later, an opposite thruster fires, causing the polhode to recross the separatrix on the desired side.

To avoid the necessity for additional sensors onboard the spacecraft, the on-orbit rate gyros, nominally used for station-keeping, are used for spin polarity control. Unfortunately, these gyros have limited range and are not designed to measure the relatively high rates that occur during spin transition. Therefore, they are only useful for determining the signs of the principal axis spin rates.

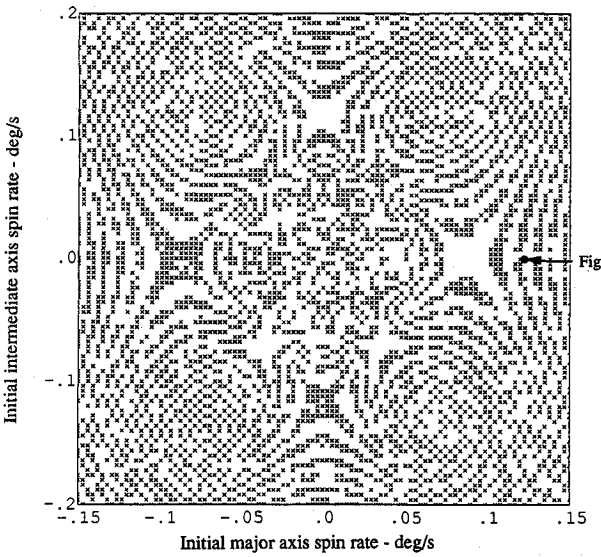

Figure 1

Fig. 2 Spin polarity from initial conditions, constant angular momentum (3000 Nms). A grid of 101 × 101 simulations shows either a positive (x) or negative (blank) major axis spin after transition starting from initial ω_1 and initial ω_2.

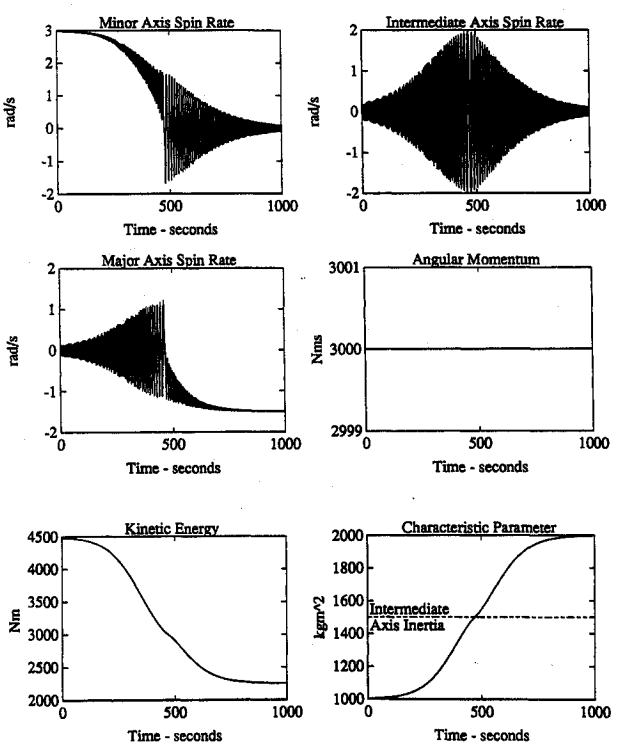

Fig. 3 Time response of spacecraft rates ω_1, ω_2, and ω_3, angular momentum h_v, kinetic energy T_v, and characteristic parameter I_v during spin transition.

Separatrix Crossing

Although predicting when the polhode will cross the separatrix is very difficult, it is relatively easy to determine that the crossing has occurred. Figures 3 show the simulated time response of the spacecraft rates during a spin transition. The spacecraft starts out with a positive minor axis spin and ends up with a negative major axis spin. When the minor axis spin rate changes sign, the polhode has crossed the separatrix. In all cases, the polhode crosses the separatrix before the minor axis spin rate changes sign. Therefore, the minor axis rate sign change is a conservative indicator of the separatrix crossing. Similarly, the major axis spin rate maintains a constant sign and the period of the intermediate axis spin rate begins to decrease after the separatrix crossing.

Also shown are the angular momentum h_v, which remains constant during the maneuver, the kinetic energy T_v, which decreases during the maneuver, and the characteristic parameter I_v, which is defined as

$$I_v = h_v^2/2T_v \tag{6}$$

Once the polhode has crossed the separatrix, the sign of the major axis spin rate can be determined from the gyros. If the sign corresponds to the desired spacecraft orientation, the maneuver is complete. If the sign is of opposite polarity, however, the spacecraft must be reoriented.

Thruster Firings

If the spin polarity after the polhode has crossed the separatrix is correct, no thrusters are fired. If it is incorrect and there are no thruster failures, two thruster firings are required to change the spin polarity. The objective of each of the two firings is to make the polhode cross the separatrix in a desired direction. This section discusses the effect of thruster firings on the characteristic parameter I.

The distance between the polhode and the separatrix is measured by the characteristic parameter

$$I = h^2/2T \qquad (I_3 \le I \le I_1) \tag{7}$$

As the energy of the body decreases, I increases. At the separatrix crossing, $I = I_2$, as seen in Figs. 3. The characteristic parameter qualitatively divides the motion into a regime of primarily minor axis spin ($I < I_2$) and primarily major axis spin ($I > I_2$).

Defining K as the equivalent gain of the thruster firing,

$$I^+ = KI \tag{8}$$

where I^+ is the characteristic parameter after the firing. If $I < I_2$, and the objective of the firing is to cross the separatrix, then K is chosen >1 such that $I^+ > I_2$. This is called an in-cross firing because the firing moves the polhode across the separatrix in the same direction as energy dissipation. For a separatrix crossing in the opposite direction (out-cross), K is chosen <1.

The equivalent gain is calculated from the thruster impulses i_1, i_2, and i_3 by assuming the thruster firings are impulsive. Substituting Eqs. (41) and (42) in Hughes[8] into Eq. (8) via Eq. (7) yields

$$K = \frac{h^2 + 2(h_1 i_1 + h_2 i_2 + h_3 i_3) + i_1^2 + i_2^2 + i_3^2}{h^2 + 2[(I_2/I_1)h_1 i_1 + h_2 i_2 + (I_2/I_3)h_3 i_3] + (I_2/I_1)i_1^2 + i_2^2 + (I_2/I_3)i_3^2} \tag{9}$$

where h_1, h_2, and h_3 are the components of the angular momentum prior to the firing.

For a given K, the timing and direction of the thruster impulse must be determined. Since the rate gyros provide only rate sign information, the thrusters must be timed according to when the sign of a rate changes, indicating the rate is zero. Combined with the three possible impulse directions, there are nine combinations of impulse direction and firing time. For most practical cases, an impulse about the minor axis that is fired when $\omega_2 = 0$ uses the least propellant for a given K. The size of the impulse can be calculated by substituting $\omega_2 = 0$, $i_1 = 0$, and $i_2 = 0$ into Eq. (9) and solving for i_3:

$$i_3 = -h_3 + \text{sgn}(h_3)\sqrt{h_3^2 - \frac{I_3 h^2(1-K)}{I_3 - KI_2}} \tag{10}$$

where sgn(x) is the sign of x.

The polhode is near the separatrix when each impulse is fired so

$$\omega_1 \approx s_1\omega_{1m}\,\text{sech}\tau \tag{11a}$$

$$\omega_2 \approx s_2\omega_{2m}\tanh\tau \tag{11b}$$

$$\omega_3 \approx s_3\omega_{3m}\,\text{sech}\tau \tag{11c}$$

where $s_1\omega_{1m}$, $s_2\omega_{2m}$, and $s_3\omega_{3m}$ are the signed amplitudes of the angular rates and τ is proportional to time.[8] The intermediate axis spin rate is zero so $\tanh\tau = 0$ and $\text{sech}\tau = 1$, resulting in

$$\omega_3 \approx s_3\omega_{3m} = s_3 h\sqrt{\frac{I_1 - I_2}{I_2 I_3(I_1 - I_3)}} \tag{12}$$

Substituting Eq. (12) into Eq. (10) yields

$$i_3 = h\,\text{sgn}(\omega_3)\{\sqrt{C_1 + C_2} - \sqrt{C_1}\} \tag{13}$$

where

$$C_1 = \frac{I_3(I_1 - I_2)}{I_2(I_1 - I_3)} \tag{14a}$$

$$C_2 = \frac{I_3(K-1)}{I_3 - KI_2} \tag{14b}$$

Polhode Path

The polhode path affected by the spin polarity control logic is shown in Fig. 4. The polhode is folded away from the inertia ellipsoid and projected onto a plane. The separatrix resembles a figure eight and the angular rates are zero on vertical and horizontal lines. The horizontal line through the middle corresponds to $\omega_3 = 0$, and the vertical lines alternate between $\omega_1 = 0$ and $\omega_2 = 0$.

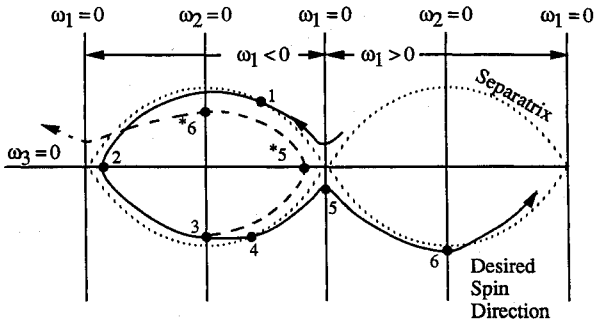

Fig. 4 Diagram of the polhode path with spin polarity control. The nominal path (plain) and the thruster failure path (dashed) are shown.

A typical polhode path is shown in-crossing the separatrix at point 1. The polhode passes through zero ω_3 at point 2. The sign of ω_1 determines that the spin direction is negative, the

opposite of the desired direction. At point 3, when ω_2 is zero, a thruster fires to decrease I ($K<1$) and the polhode outcrosses the separatrix at point 4. The polhode then crosses $\omega_1 = 0$ (point 5), and when $\omega_2 = 0$ (point 6), a thruster fires to increase I($K>1$) by the same amount as it was decreased in the previous firing, thus ensuring capture on the desired side.

Choosing K

The parameter K calculates the thruster impulse required to push the polhode across the separatrix. When selecting this parameter, the rate of energy dissipation and the limits of the impulsive approximation must be considered.

To ensure that the first firing forces the polhode to outcross the separatrix, it must compensate for the energy lost since the polhode in-crossed the separatrix. In the worst case, the polhode in-crosses the separatrix a half period from when ω_3 crosses zero, and so by the time ω_2 is zero and the thruster is fired, 3/4 of a period has elapsed.

Designating Δt as the time from $\omega_3 = 0$ to $\omega_2 = 0$, the worst case I at the first thruster firing would be

$$I = I_2 + 3\Delta t \left(\frac{\partial I}{\partial t}\right)_{\text{separatrix}} \tag{15}$$

The desired I^+ should be large enough to ensure the separatrix is not in-crossed before $\omega_1 = 0$ a quarter period later, or

$$I^+ = I_2 - \Delta t \left(\frac{\partial I}{\partial t}\right)_{\text{separatrix}} \tag{16}$$

Substituting Eqs. (15) and (16) in Eq. (8) and utilizing Eq. (7) yields

$$K = \frac{1 + \Delta t[(1/T)(\partial T/\partial t)]_{\text{separatrix}}}{1 - 3\Delta t[(1/T)(\partial T/\partial t)]_{\text{separatrix}}} \tag{17}$$

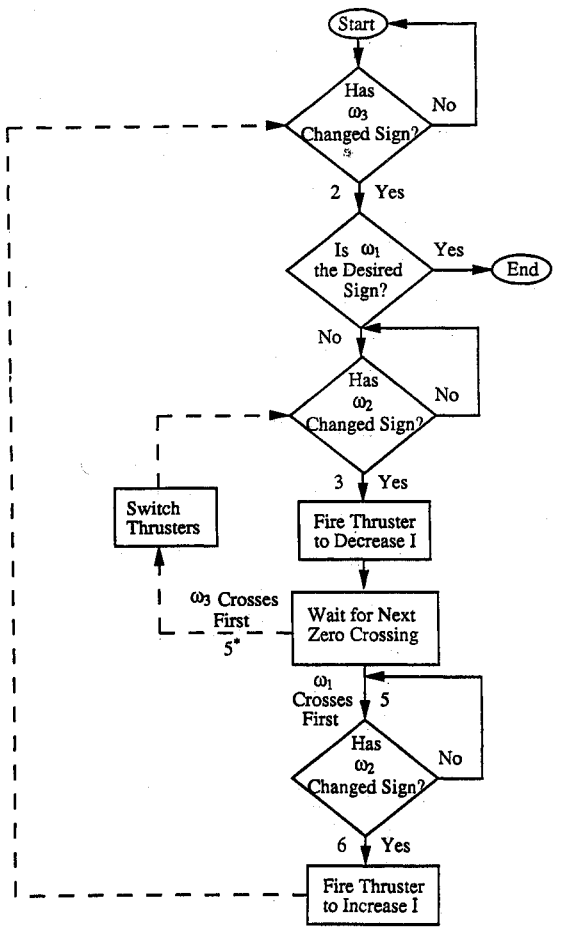

Fig. 5 Control logic flow diagram.

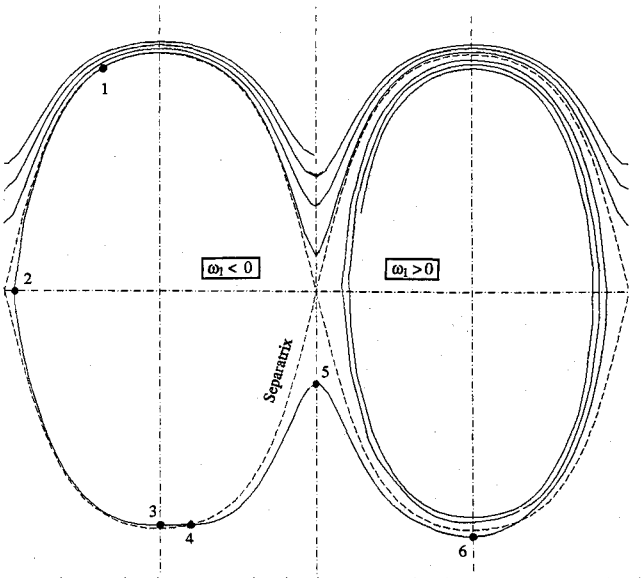

Fig. 6 Polhode path simulation with spin polarity control. The polhode plot is projected onto a plane showing both the positive and negative final spin polarity regions.

In order to calculate K from Eq. (17), the energy dissipation characteristics of the spacecraft at the separatrix must be known. These characteristics can be determined experimentally[9] or from the telemetry data of a spacecraft with similar energy dissipation characteristics. If there is some uncertainty in the energy dissipation, a larger impulse can be used.

Each of the two firings is the same in magnitude and opposite in direction. In practice, however, the second firing can be smaller than the first. After the first firing, the energy dissipation moves the polhode in the same direction as the desired separatrix in-crossing of the second firing. When the second thruster fires, the polhode is closer to the separatrix than it was for the first firing and a smaller impulse can be used.

The initial angular momentum of the spacecraft must be compatible with the thruster size, configuration, and minimum impulse bit. The size and configuration of the thrusters limit the maximum torque T_3. The impulse i_3 equals T_3 times the firing time. If T_3 is small, a longer firing time is required, invalidating the impulsive approximation. This results in lost efficiency, and the desired I^+ may not be achieved. If the thruster is fired when ω_2 changes sign, the firing must be finished by the time ω_3 changes sign, otherwise the firing will not produce the desired effect. Reducing the initial spin rate contracts the thruster firing time proportionally [see Eq. (13)], alleviating this problem. Alternatively, if the minimum angular impulse of the thrusters is large compared to h, fuel will be wasted.

Control Logic Description

Figure 5 shows the flow diagram for the control logic. Initially, the control system monitors the ω_3 rate from the gyro. When ω_3 changes sign, the sign of the saturated ω_1 gyro rate is measured. If this rate has the desired sign, the spin transition has been successfully completed. Therefore, there is a 50% chance that the controller will take no action. If the rate is of opposite sign, however, the controller waits for a change in sign of ω_2 and fires a thruster that reduces I according to Eq. (13). The control system then waits for the zero crossing of ω_1 followed by a change in polarity of ω_2 and then fires a torque about the minor axis to guarantee capture.

Figure 6 shows the simulated polhode path for a controlled spin transition with the same initial conditions and mass properties as in Fig. 1. The control system is configured to ensure a positive final spin rate. The polhode first crosses the separatrix at point 1. When ω_3 is zero (point 2), ω_1 is less than zero.

When ω_2 crosses zero (point 3), a thruster is fired and the polhode out-crosses the separatrix at point 4. Next, ω_1 crosses zero (point 5), signaling successful completion of the separatrix crossing. At point 6, ω_2 crosses zero, the second firing increases I, and the polhode captures on the desired side.

Figures 7 show the time response of the angular rates h_v, T_v, and I_v. The ω_1 response initially captures on the negative side and then is pushed by thruster firings to the positive side. The angular momentum and kinetic energy change each time a thruster fires with the parameter I_v decreasing and then increasing. After the second firing, h_v differs slightly (0.33%) from its initial value. This difference is due to the limitations in the analysis model and assumptions; namely, the impulsive approximation, ignoring the slug dynamics, and assuming the polhode is on the separatrix when the thruster is fired.

Autonomous Thruster Failure Detection

The dashed polhode path in Fig. 4 would be followed if the thruster used for the first firing had failed. In that case, the ω_3 gyro rate will cross zero (point 5*) before the ω_1 gyro rate. If this happens, the control system switches autonomously to a backup string of thrusters and fires a larger impulse at point 6*.

The dashed lines in Fig. 5 show the autonomous thruster failure detection logic. After the first firing, the controller monitors both the ω_1 and ω_3 rates. If ω_1 crosses first, then the nominal logic is followed. If ω_3 crosses first then the thrusters are reconfigured and a larger impulse is fired. The dashed path after the second firing ensures that the second thruster has not failed. In practice, the number of passes through the flow diagram is limited to preclude the possibility of limit cycles.

Gyro Misalignment

More accurate gyro models include small misalignments and nonzero ranges. The measured gyro rates ω_{si} are related to the actual angular velocities

$$\omega_{si} = \begin{cases} \Sigma_{j=1}^{3} C_{ij}\omega_j & \text{if } |\Sigma_{j=1}^{3} C_{ij}\omega_j| < \omega_{si}^{\max} \\ \omega_{si}^{\max}\ \mathrm{sgn}(\Sigma_{j=1}^{3} C_{ij}\omega_j) & \text{otherwise} \end{cases} \tag{18}$$

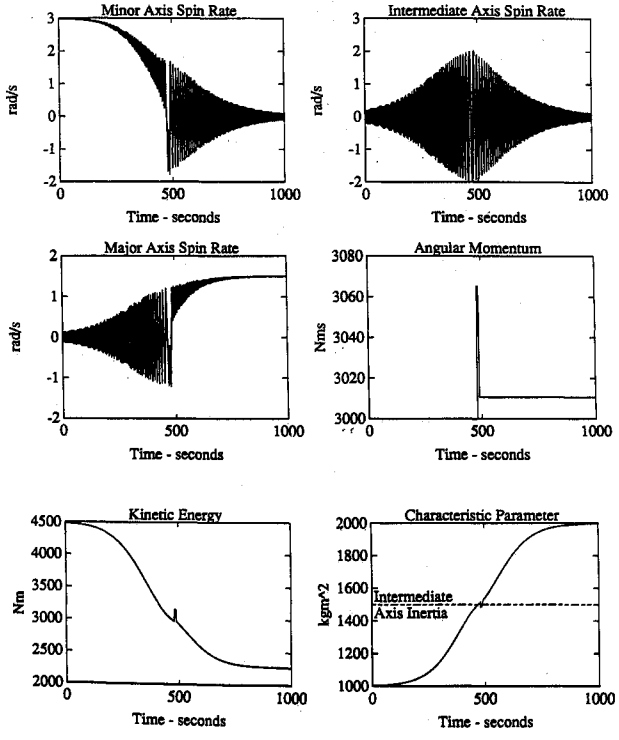

Fig. 7 Controlled time response of spacecraft rates, angular momentum, energy, and characteristic parameter during spin transition. The desired, positive major axis spin rate is achieved.

where C_{ij} are the direction cosines and $\omega_{si}^{\max}$ are the saturation levels of the gyros. Small gyro misalignment implies $C_{ii} > C_{ij} (i \neq j)$.

With misaligned gyros, the proposed control logic must be modified. Instead of using sign changes of ω_1, ω_2, and ω_3 to determine thruster firings, sign changes of $\omega_{si} - \omega_{ti}$ ($|\omega_{ti}| \leq \omega_{si}^{\max}$) must be used.

Consider, for example, the first separatrix crossing, which is determined by a change in sign of ω_3. The modified logic looks for a sign change in $\omega_{s3} - \omega_{t3}$. Since the ω_{s3} gyro measures predominantly ω_3, sign changes are most likely to occur near the separatrix, when ω_3 is minimum and ω_1 and ω_2 are maximum. On the separatrix

$$\omega_{3s} = (C_{33}s_3\omega_{3m} + C_{31}s_1\omega_{1m})\ \mathrm{sech}\tau + C_{32}s_2\omega_{2m}\ \tanh\tau \tag{19}$$

where Eqs. (11) have been used. The first term is the same sign as ω_3 if $|C_{33}\omega_{3m}| > |C_{31}\omega_{1m}|$, or, substituting for ω_{1m} and ω_{3m},

$$|C_{33}| > |C_{31}| \left[\frac{(I_2 - I_3)I_3}{(I_1 - I_2)I_1}\right]^{1/2} \tag{20}$$

With $|C_{33}| > |C_{31}|$ and $I_3/I_1 < 1$, this requirement is met for most cases. When $\omega_3 = 0$, $\omega_{3s} = C_{32}s_2\omega_{2m}$. Correspondingly,

$$\omega_{3t} = C_{32}s_2\omega_{2m} = \frac{C_{32}s_2 h}{I_2} \tag{21}$$

The sign of ω_2 (s_2) is measured from the sign of ω_{s2}. At the $\omega_3 = 0$ crossing, $\omega_{s2} \approx \omega_2$ and $\omega_1 \approx \omega_3 \approx 0$, which implies that $\mathrm{sgn}(\omega_{s2}) = s_2$. In order to keep $|\omega_{3t}| < \omega_{s3}^{\max}$, it may be necessary to reduce h.

Conclusions

The spin transition maneuver, when augmented with two thruster firings based on gyro measurements, provides a predetermined final spin polarity. The control logic utilizes rate sign changes to determine when the separatrix has been crossed and when thrusters must be fired. The sizing of the thruster firings is based on estimates of the energy dissipation in the spacecraft. Limitations in the torque capability of the thruster configuration or gyro misalignment may constrain the maximum initial spin rate that can be controlled.

Acknowledgments

The authors would like to thank C. D. Mote Jr. for the use of his computational facilities and Jonathan Wickert for his useful discussions on chaos.

References

[1]Likins, P. W., "Effects of Energy Dissipation on the Free Body Motions of Spacecraft," NASA TR 32-860, July 1966.

[2]Thomson, W. T., *Introduction to Space Dynamics*, Wiley, New York, 1961, pp. 220–227.

[3]Leliakov, I. P., and Barba, P. M., "Damping Spacecraft Nutation by Means of a Despun Antenna," AAS/AIAA Astrodynamics Conference, Vail, CO, July 1973.

[4]Junkins, J. L., and Turner, J. D., *Optimal Spacecraft Rotational Maneuvers*, Elsevier, New York, 1986.

[5]Weissberg, J., and Ninomiya, K., "Improved Method for the Initial Attitude Acquisition Maneuver," *Journal of Guidance, Control, and Dynamics*, Vol. 10, No. 3, 1987, pp. 316–319.

[6]Hubert, C., "Spacecraft Attitude Acquisition from an Arbitrary Spinning or Tumbling State," *Journal of Guidance, Control, and Dynamics*, Vol. 4, No. 2, 1981, pp. 164–170.

[7]Barba, P. M., Hooker, W. W., and Leliakov, I. P., "Parameter Selection for a Class of Dual Spin Satellites," Symposium on Attitude Stability and Control of Dual-Spin Spacecraft, Aerospace Corporation, TR-0158 (3307-01)-16, Aug. 1967.

[8]Hughes, P. C., *Spacecraft Attitude Dynamics*, Wiley, New York, 1986, pp. 104–108.

[9]Harrison, J. A., Garg, S. C., and Furumoto, N., "A Free-Fall Technique to Measure Nutation Divergence, and Applications," AIAA Paper 83-372, Aug. 1983.